minerals

MDPI

Article

A New Experimental Approach to Improve the Quality of Low Grade Silica; The Combination of Indirect Ultrasound Irradiation with Reverse Flotation and Magnetic Separation

Hamed Haghi *, Mohammad Noaparast, Sied Ziaedin Shafaei Tonkaboni and Mirsaleh Mirmohammadi

School of Mining Engineering, University of Tehran, North Karegar St, Jalal-Ale-Ahmad Hwy, College of Engineering, Tehran 1439957131, Iran; noparast@ut.ac.ir (M.N); zshafaie@ut.ac.ir (S.Z.S.T); m.mirmohammadi@ut.ac.ir (M.M)

* Correspondence: hhaghi@ut.ac.ir; Tel./Fax.: +98-21-8800-8838

Academic Editor: Massimiliano Zanin

Received: 14 July 2016; Accepted: 3 November 2016; Published: 10 November 2016

Abstract: Removal of iron impurities in silica is one of the most important issues in the glass industry. The most noted impurities are surface coating and staining on silica particles; additionally, some cases of inclusions are observed. The prepared silica sample, for this research work, mostly was in the size range of 106–425 μm. Mineralogical studies indicated the existence of goethite, hematite, limonite and pyrite as the major iron impurities. The poor liberation degree of silica particles from clays encouraged the use of ultrasound irradiation to improve the efficiency of reverse flotation. The head sample contained 96.98% SiO_2, 0.143% Fe_2O_3, 1.52% Al_2O_3, and 0.088% TiO_2; Fe_2O_3 had to be reduced to below 0.04%. The reverse flotation tests were carried out with and without indirect ultrasound irradiation. The lowest Fe_2O_3 grade of the flotation yield was 0.058% and this was achieved using 2000 g/t of C_4 collector with 15 min conditioning at neutral pH. C_4 consisted of Aero 801, Aero 825, oleic acid and sodium oleate at equal dosage. As a result, a flowsheet was developed to include indirect ultrasound irradiation with reverse flotation and two stages of dry high intensity magnetic separation. In conclusion, the best product contained 98.43% SiO_2, 0.034% Fe_2O_3, 0.90% Al_2O_3 and 0.051% TiO_2.

Keywords: silica; iron removal; ultrasound irradiation; reverse flotation; magnetic separation

1. Introduction

Silica is an important product in industrial minerals and it has many applications. Silica with low iron content is much in demand for glass, ceramics, and pottery use [1]. Different silica deposits are used in the production of a high purity silica product and they can be classified as three main types [1]:

1. Quartz veins: These deposits are extremely high-grade containing white silica crystals.
2. Quartzite: This is metamorphosed sandstone made up chiefly of quartz sand united by siliceous cement, forming low-porosity rock. Quartzite varies from white to gray in color and sometimes brown, red, or yellow due to the presence of small amounts of impurities. Some quartzite deposits may contain up to 99% SiO_2.
3. Sandstone deposits: These deposits contain significant amounts of impurities and may contain clay, in the range of 5%–10%. The origin of these deposits is Paleozoic sediment.

Silica is the most important raw material in the glass industry. The silica used in the glass industry should have certain physical properties such as a special particle size distribution (normally finer than

600 μm and mostly present in the size range of 100–420 μm), less than 2% of fine particles (<100 μm) and chemical properties like the percentage of major oxides including SiO_2, Al_2O_3, Fe_2O_3, Cr_2O_3, and TiO_2. In general, the occurrence of iron impurities in such raw materials is undesirable for glass manufacturing. The target iron oxide grade in silica varies depending on the glass type, and, according to Table 1, it is about 0.1% and less than 0.04% for clear flat (float) glass and colorless glass containers, respectively [2].

Table 1. Specifications of silica for glass-making sands [2].

Application & Description	Chemical Composition (%)			
	SiO_2	Al_2O_3	Fe_2O_3	Cr_2O_3
Optical & ophthalmic glass	>99.7	<0.2	<0.013	<0.00015
Tableware & lead crystal glasses	99.6 ± 0.1	0.2 ± 0.1	≤0.01	<0.0002
Borosilicate glasses	99.6 ± 0.1	0.2 ± 0.1	≤0.010	0.0002
Colorless glass containers	98.8 ± 0.2	Nominal ± 0.1	≤0.03 ± 0.003	0.0005
Clear flat glass	99.0 ± 0.2	0.5 ± 0.15	0.10 ± 0.005	-
Colored glass containers	97.0 ± 0.3	Nominal ± 0.1	0.25 ± 0.03	-
Glass for insulating fibers	94.5 ± 0.5	3.0 ± 0.5	0.3 ± 0.05	-

The samples were taken from the process line of a plant that produces silica as a raw material for flat glass manufacturing. The objective of this research work was to remove the impurities including clays, carbonates and most of the iron content from relatively low grade silica, in order to meet the minimum requirements for manufacturing colorless glass containers. The head sample contained 96.98% SiO_2 and 0.143% Fe_2O_3 and the target was to reduce Fe_2O_3 down to below 0.04% and improve the SiO_2 grade to around 98.5% at the same time; therefore, a new experimental approach was developed including indirect ultrasound irradiation with reverse flotation followed by dry high intensity magnetic separation.

1.1. Enrichment of Silica Used in the Glass Industry

The iron content can be reduced by a number of physical, physicochemical or chemical methods. The most appropriate methods are determined depending on the mineralogical forms and distribution of iron in the ore [3,4]. The silica purification process can start with preliminary crushing including jaw and cone crushers, and wet milling followed by size classification in a teetered bed separator (TBS). TBS normally works in a closed circuit with the mill to improve the partition curve of ground silica and reduce the generation of higher amounts of slimes [3,5]. Afterwards, the enrichment process can be continued with attrition scrubbing by applying different chemical reagents such as caustic soda (NaOH) [1], sodium carbonate (Na_2CO_3) [4], hydrochloric acid (HCl) and sodium dithionite ($Na_2S_2O_4$) [6] or sulfuric acid [1,7]. The process can be followed by gravity separation, employing a shaking table or spiral concentrator [8,9], and at the same time using spiral concentrators for rejecting aluminum silicates and mica from quartz particles designed for glass making markets. In addition, it should be noted, in some cases, spiral separation is both cost effective and environmentally friendly when compared with other techniques for iron bearing and heavy mineral elimination, such as reverse flotation and magnetic separation [8]. Another study for treating relatively low grade silica deposits proved that gravity separation was not enough and a combination of attrition scrubbing, gravity separation, reverse flotation and finally high intensity magnetic separation should be employed. As a result, with the aforementioned combined processes, the iron content (Fe_2O_3 grade) was reduced to less than 0.1% and the silica grade was upgraded to 98.9% [10]. Other studies confirmed that combining attrition scrubbing with dry high intensity magnetic separation (DHIMS), or a combination of attrition scrubbing and spiral concentration with DHIMS, can result in the production of silica with less than 0.05% Fe_2O_3 [7,11,12]. When the objective of enrichment is to produce high purity silica from relatively low grade feed (generally 94% < SiO_2 < 98%), the use of reverse flotation in the processing

circuit is unavoidable [12–16]. Some silica deposits contain impurities such as pyrite, iron oxides, and feldspar. Purification of silica from these deposits involves attrition scrubbing followed by a three-stage flotation process (for removal of pyrite, iron oxides and feldspar separately) [1]. In addition, there are recorded efforts to improve iron removal from silica by using Cyclojet or pneumatic flotation cells [15,16]. The last step for iron removal from silica is leaching, and many works have been conducted to investigate iron removal from silica [17–21]. It should be mentioned that some efforts were made to remove iron from relatively low grade silica using different reagents (H_2SO_4, HCl, and oxalic acid) in leaching experiments [1,6,22,23].

1.2. Application of Ultrasound Irradiation in Mineral Processing

In the recent decade, the application of ultrasound irradiation in mineral processing has been increasingly used. Sound travels through a fluid in a three-dimensional pressure wave form, consisting of alternating cycles of compression and rarefaction. The frequency range of 16 Hz–16 kHz covers the audible range; however, the frequency range of 20–100 kHz is commonly used for ultrasound irradiation [24–26]. Ultrasound irradiation is one of the important pretreatment methods which are notably reported and used to enhance flotation performance [27–31]. The main effects of ultrasonic vibration in liquids are acoustic cavitation and acoustic streaming. Cavitation occurs due to implosion of bubbles in the acoustic field and the resulting transmission of shock waves. The violent collapse of the cavitation bubbles results in a specific environment with extremely high temperature (5000 K) and pressure of up to 1000 atm [24–26]. The occurrence of ultrasonic cavitation depends on a number of factors including temperature, surface tension, medium viscosity, hydrostatic pressure, the degree of gas saturation, gas type and a few other minor factors; therefore they are various for different mediums and experimental conditions [24,32,33]. Acoustic streaming is caused by unidirectional flow of currents in a fluid as a consequence of sound waves [34]. The main advantage of ultrasound irradiation compared to conventional attrition scrubbing is that it allows penetration into available surface microscopic cracks. This procedure helps loosen the bonded iron minerals and possible other contaminating impurities [13,24–26,35,36].

2. Materials and Methods

2.1. Sample Recognition and Mineralogical Study

The silica samples were provided from a silica processing plant located near Abhar city in the Zanjan province of Iran. According to Figure A1, these samples were gathered from two points: the outlet of the crushing stage (CSP) and the underflow of the TBS, which is de-slimed by the hydro-cyclone (PPHS). The chemical composition of these two samples is provided in Table 2. According to Table 2 and comparing the CSP and PPHS samples with the silica quality of former research, it is postulated that this silica is one of the poorest quality silica samples that have ever been examined. This is due to the high grades of Fe_2O_3, Al_2O_3, K_2O and CaO. It is important to note that the chemical composition of the PPHS sample was investigated using different methods, including X-ray fluorescence spectrometer (XRF, Magix PRO-PW 2440 model, Philips, Amsterdam, The Netherlands), inductively coupled plasma optical emission spectrometry (ICP-OES, Optima 4100 DV model, Perkin Elmer, Waltham, MA, USA) and chemical analysis (CA) (i.e., gravimetric and titration approaches, as well as spectrophotometer and flame photometer methods). After preliminary preparation, the head sample (PPHS) was washed and classified into six size fractions. Then samples were prepared for chemical analysis and mineralogical studies. Chemical analyses of the major components in the different size fractions are presented in Table 3. According to Table 3, there is an incremental trend in Al_2O_3, Fe_2O_3, and TiO_2 grades when particle size decreases while the reverse trend is observed for silica grade. At the same time, there was no significant trend in K_2O and CaO grades for the different size fractions.

Table 2. Chemical composition of the head sample and comparison with former studies.

Type/Description		SiO_2	Fe_2O_3	Al_2O_3	TiO_2	K_2O	CaO	MgO	LOI	Na_2O	P_2O_5	SO_3
White Sand [a]		99.7	0.025	0.08	0.02	0.005	0.01	0.01	0.126	0.004	-	-
Yellow Sand [a]		99.1	0.15	0.25	0.05	0.05	0.01	0.01	0.365	0.015	-	-
Badgeley Island [b]		98.5	0.04	0.8	0.02	0.14	0	0.03	0.16	0.01	0.01	-
Shequiandah [b]		97.90	0.08	0.8	0.05	0.3	0.04	0.07	0.24	0.1	0.03	-
Grenville Quartzite [b]		96.90	0.22	0.68	0.06	0.09	0	0.03	0.12	0.01	0.01	-
Aydin-Cine, Turkey [c]		94.81	0.137	2.94	0.035	0.62	0.09	0.06	0.54	0.77	-	-
Florinas quarry, Italy [d]		98.95	0.011	0.40	-	0.33	0.18	-	-	0.13	-	-
Greece [e]		98.01	0.066	0.37	0.48	0.037	0.097	0.018	0.883	0.032	-	-
Greece [e]		96.85	0.189	0.62	0.41	0.07	0.038	0.039	1.72	0.058	-	-
Sandstone, Algeria [f]		97.20	0.62	1.04	0.22	0.01	0.09	0.1	0.44	0.26	-	0.02
White Sand, Egypt [g]		99.44	0.046	0.044	0.030	0.01	0.060	0.020	0.30	0.01	0.01	0.01
Aghires, Romania [h]		97.77	0.18	1.29	0.28	-	-	-	0.45	-	-	-
CSP [1]	ICP-OES [3]	95.58	0.27	2.37	0.1	0.53	0.22	0.1	0.72	0.02	0.02	0.07 *
	XRF [4]	97.28	0.123	1.17	0.09	0.392	0.203	0.052	0.673	-	0.015	0.002
PPHS [2]	ICP-OES	97.43	0.134	1.20	0.07	0.416	0.213	0.070	0.450	-	0.010	0
	CA [5]	96.98	0.143	1.52	0.088	0.402	0.467	-	0.40	-	-	-

[a] From Reference [37]; [b] From Reference [38]; [c] From Reference [13]; [d] From Reference [19]; [e] From Reference [39]; [f] From Reference [40]; [g] From Reference [9]; [h] From Reference [16]; [1] CSP: Crushing Stage Product; [2] PPHS: Processing Plant Head Sample; [3] Average grades of two separate analyses applying lithium borate fusion and using ICP-OES (inductively coupled plasma optical emission spectrometry); [4] Average grades of three separate analyses using XRF (X-ray fluorescence) spectrometer; [5] Average grades of seven separate analyses using chemical analysis (CA); * including SO_3 + BaO + MnO + Cr_2O_3.

Table 3. Chemical analysis of major components in the size fractions of the head sample.

Size Range (μm)	Average Size (μm)	wt %	Major Components						
			SiO_2	Fe_2O_3	Al_2O_3	TiO_2	K_2O	CaO	LOI *
420–600	502.0	15.75	96.97	0.088	1.68	0.060	0.33	0.41	0.51
300–420	355.0	28.33	97.20	0.088	1.13	0.071	0.33	0.42	0.65
212–300	252.2	18.62	96.96	0.104	1.45	0.105	0.35	0.39	0.55
150–212	178.3	23.89	96.81	0.127	1.74	0.122	0.36	0.44	0.67
106–150	126.1	9.88	96.64	0.133	1.90	0.089	0.43	0.50	0.60
75–106	89.2	3.52	94.40	0.365	2.30	0.176	0.41	0.56	0.98
Head **	284.8	100	96.87	0.114	1.54	0.093	0.35	0.43	0.60

LOI: Loss on ignition; * Based on average results of X-ray fluorescence analysis; ** Calculated grades.

Mineralogical studies were carried out through investigating macroscopic CSP samples and conducting microscopic studies on thin and polished sections which were prepared from different size fractions of the head sample. A summary of the mineralogical studies for different size fractions and the relevant liberation degree of impurities from silica particles is presented in Table 4. It should be noted that the liberation degree of silica particles from impurities was calculated via the ratio of counted liberated silica particles versus the total number of counted particles in each selected section. This silica ore was quartzite and the main iron impurities were goethite, hematite, limonite and pyrite. There are four sources of iron impurities, which can be classified as follow:

1. Goethite and hematite altered from primitive pyrite, and liberated from quartz crystals; it is easy to separate these types of impurities from silica utilizing spiral concentration, reverse flotation or magnetic separation.
2. Surface staining and coating of silica particles with iron hydroxides (goethite, hematite and limonite); attrition scrubbing and ultrasound irradiation when using chemical reagents can separate these impurities from silica.
3. Filled voids, cracks and fractures with carbonates and iron impurities; acidic leaching and washing or carbonates flotation can separate these two impurities from silica particles.
4. Ultra-fine iron impurities (even finer than 10 μm) in the form of unchanged pyrite as inclusions inside quartz particles; this is the worst type of iron impurities in this sample and it is difficult to separate them from quartz.

Table 4. Summary of mineralogical studies for different size fractions.

Size Range (μm)	wt. %	Major Iron Minerals	Major Nonmetallic Impurities	Average Liberation Degree from Silica Particles		
				Iron Impurities	Clays	Carbonates
420–600	15.75	Gt > Hem >> Py	Ill ≈ Kln > Cal >> Fsp	25	17.5	57.5
300–420	28.33	Gt > Lm >> Hem >> Py	Ill ≈ Kln > Cal > Mca >> Fsp	45	35	75
212–300	18.62	Gt ≈ Lm > Hem >> Py	Ill ≈ Kln > Cal > Mca >> Fsp	57.5	40	80
150–212	23.89	Gt > Lm > Hem >> Py	Kln > Ill > Cal >> Fsp	80	50	85
106–150	9.88	Gt > Hem >> Py	Kln > Ill > Cal > Fsp >> Mca	85	52.5	90
75–106	3.52	Gt > Hem >> Py	Kln > Ill > Cal > Fsp >> Mca	87.5	57.5	95
Average liberation degree of head sample				57.99	39.28	77.75

Calcite (Cal); Feldspar (Fsp); Goethite (Gt); Hematite (Hem); Illite (Ill); Kaolinite (Kln); Limonite (Lm); Mica (Ms); Pyrite (Py).

According to Table 4, the liberation degree of silica particles from iron impurities was more than 80% in the size range of 150–212 μm and the average liberation degree of the head sample was about 58%.

X-ray diffraction (XRD) analysis was carried out using a D8-Advance diffractometer (Bruker AXS, Karlsruhe, Germany). Figure 1 shows the XRD pattern of the head sample.

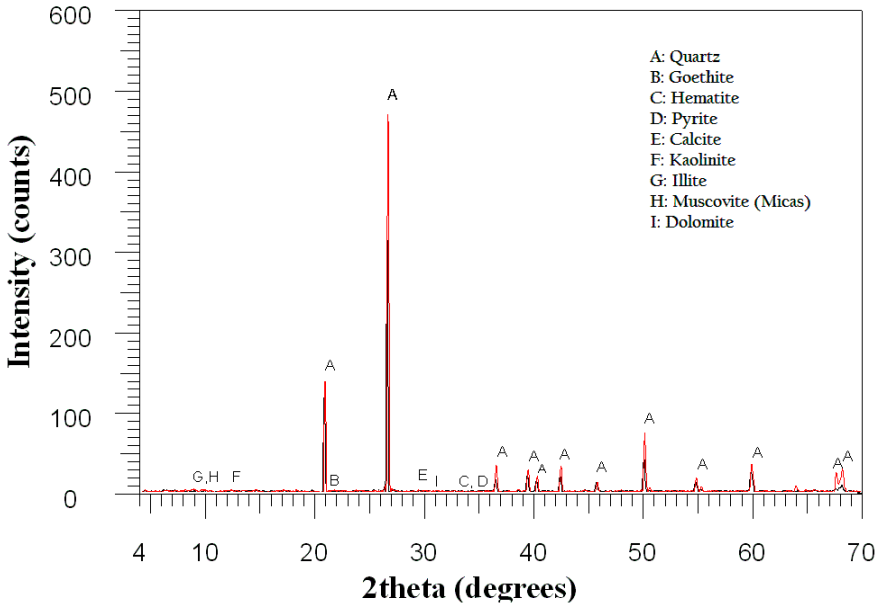

Figure 1. X-ray diffraction (XRD) pattern of the head sample.

Non-metallic impurities in the head sample can be summarized as follow:

1. Clay minerals including kaolinite and illite mostly attached to quartz particles with poor liberation degree, including silica particle sizes below 100 µm; therefore, the average liberation degree was low and around 40% (Table 4).
2. Carbonates, mainly calcite and rarely dolomite, were mostly liberated from quartz particles and the average liberation degree was around 78% (Table 4).
3. Other minor non-metallic impurities were feldspars (mostly microcline and sanidine) and micas (muscovite, biotite and sericite) while tourmaline and zircon were identified as trace non-metallic impurities.

2.2. Experimental Procedure

Former studies proved that a process including reverse flotation followed by high intensity magnetic separation is the best way for purifying the relatively low grade silica [12,14,16]. Therefore, the aforementioned process was considered in the development of a new enrichment circuit.

2.2.1. Ultrasound Irradiation

To investigate the effect of ultrasound irradiation in reverse flotation experiments, the setup in Figure 2a was designed by combining indirect ultrasound irradiation and a conventional Denver D12 flotation cell. A Sono ultrasonic bath (SW6H model) was utilized with internal tank dimensions of 300 mm × 151 mm × 150 mm, a frequency of 38 kHz and maximum ultrasonic power of 150 Watt for indirect ultrasound irradiation during the conditioning phase of reverse flotation tests. This ultrasonic bath supplies ultrasound power via 3 ultrasonic transducers mounted at the bottom of the tank. An Efergy-Wattmeter, a Lutron TM-916 thermometer with a TP02 probe and a pH meter (pH330i model) were used for system monitoring.

2.2.2. Reverse Flotation

For the reverse flotation experiments, there were fixed and variable parameters. The fixed conditions of the reverse flotation experiments are summarized below:

Rotor speed: 1400 rpm (it is fixed for the conditioning and flotation phases)
Acidic pH modifier: H_2SO_4
Average solids percent in the reactor during ultrasound irradiation: 30.6% (by weight)
Average solids percent in the flotation cell after dilution, prior to flotation: 23.4% (by weight)
Mixing of diluted slurry prior to flotation in a two liter flotation cell: 2.5 min
Frother conditioning time prior to flotation: 2 min
Frother Type: MIBC/Pine Oil (1:1)
Flotation time: 5 min

The variable conditions for the reverse flotation experiments including measured absorbed power in different places in the ultrasonic cleaner cell are shown in Table 5. In order to find the most effective mix of collectors, in addition to previously known collectors (C_1, and C_2), three new mixed collectors (C_3, C_4, and C_5) were introduced with different weight ratios:

1. One collector (C_1): Sodium oleate
2. Two collectors (C_2): Aero 801/Aero 825 (1:1)
3. Three collectors (C_3): Aero 801+ Aero 825/Oleic acid (1:1)
4. Four Collectors (C_4): Aero 801/Aero 825/Oleic acid/Sodium oleate (1:4)
5. Five collectors (C_5): Aero 801/Aero 825/Oleic acid/Sodium oleate (5:24) + Aero 845 (4:24)

2.2.3. Magnetic Separation

The application of wet magnetic separation is easy and avoiding utilization of a dryer is an advantage. However, dry magnetic separation provides better results, including relatively lower Fe_2O_3 grade in the final product with higher silica recovery compared to wet magnetic separation [12]. On the other hand, wet high intensity magnetic separation (WHIMS) had disappointing efficiency for iron removal from silica even by increasing the magnetic field intensity up to two Tesla [11]. In addition to the technical advantage of DHIMS for iron removal from silica, utilizing a dryer can be a cost effective approach for silica when it is used in the glass industry for the following reasons:

(1) When silica is used for the glass industry, it should contain below five percent moisture. If the silica contains more moisture, it should be dried prior to melting in a glass furnace.
(2) The silica product should be transported by truck from the processing line to the glass manufacturing plant; therefore, the existence of moisture will significantly increase the transportation cost per ton.

Finally, an Exolon induced roll magnetic separator (IRMS) was also utilized in this study. The silica product from reverse flotation was dried and then treated in two stages of DHIMS using the Exolon IRMS for all 17 experiments. The operating zone of the Exolon IRMS in the cleaner stage is shown in Figure 2b. The schematic flowsheet for silica purification, combining ultrasound irradiation with reverse flotation followed by two stages of DHIMS, is shown in Figure 2c. Table 6 shows the operating conditions for the DHIMS tests, including the average weight of different streams in the rougher and cleaner stages.

Table 5. Variable conditions of the reverse flotation experiments and measured absorbed power.

No.	pH [1]	Collector				Frother Dosage (g/t)	Absorbed Power (W) *					E (%)
		Type	Dosage (kg/t)	Conditioning			Reactor			P_{Tank}	P_{PAU}	
				USI [2]	Duration (min)		ΔT (°C)	Liquid	Solid			
1	8.72	C_3	2.0	No	10	74	1.9	20.70	1.89	-	-	-
2	8.49	C_3	2.0	Yes	10	74	6.5	51.57	4.67	65.84	42.59	39.28
3	4.62	C_2	2.0	Yes	12	74	3.8	23.79	2.16	79.11	12.30	13.45
4	7.92	C_1	2.0	Yes	15	74	8	42.26	3.73	77.82	32.34	29.36
5	8.09	C_1	2.0	No	15	74	2.7	35.66	1.26	-	-	-
6	7.54	C_4	2.0	Yes	15	74	6.5	34.31	3.03	91.76	23.69	20.52
7	7.03	C_4	2.0	No	15	74	2.5	13.05	1.12	-	-	-
8	7.52	C_4	2.0	Yes	20	74	8	38.36	3.58	83.57	28.29	25.29
9	7.10	C_4	2.0	No	20	74	3.8	15.58	1.33	-	-	-
10	3.41	C_4	2.0	No	15	74	1.8	9.15	0.84	-	-	-
11	3.52	C_4	2.0	No	20	74	3.7	14.36	1.30	-	-	-
12	3.52	C_4	2.0	Yes	15	74	7.6	39.88	3.55	77.82	29.78	27.67
13	3.51	C_4	2.0	Yes	20	74	7.7	30.26	2.70	70.56	19.31	21.49
14	7.5	C_5	1.2	No	30	37	8	21.56	1.87	-	-	-
15	7.5	C_5	1.2	Yes	30	37	13.4	40.69	3.52	87.11	30.56	25.97
16	3.52	C_5	1.2	No	30	37	7.6	20.57	1.77	-	-	-
17	3.60	C_5	1.2	Yes	30	37	13.4	38.34	3.30	78.40	27.99	26.31
Average amount for all tests without ultrasound irradiation							0.19 **	19.38	1.50	-	-	-
Average amount for all tests with ultrasound irradiation							0.46 **	39.46	3.51	79.32	27.43	25.45

[1] Average measured pH during conditioning; [2] USI: Ultrasound irradiation; * Accuracy of temperature measurement was 0.1 centigrade degree (°C) and measurement errors for solid and liquid were 0.02% (0.1 g/500 g) and 0.5% (5 cc/1000 cc), respectively; P_{Tank}: Absorbed ultrasound power in the tank; P_{PAU}: Pure absorbed ultrasound power in the conditioning reactor; E: Ratio of transferred power to the reactor versus the total produced power in the ultrasonic bath; ** Average ΔT/min.

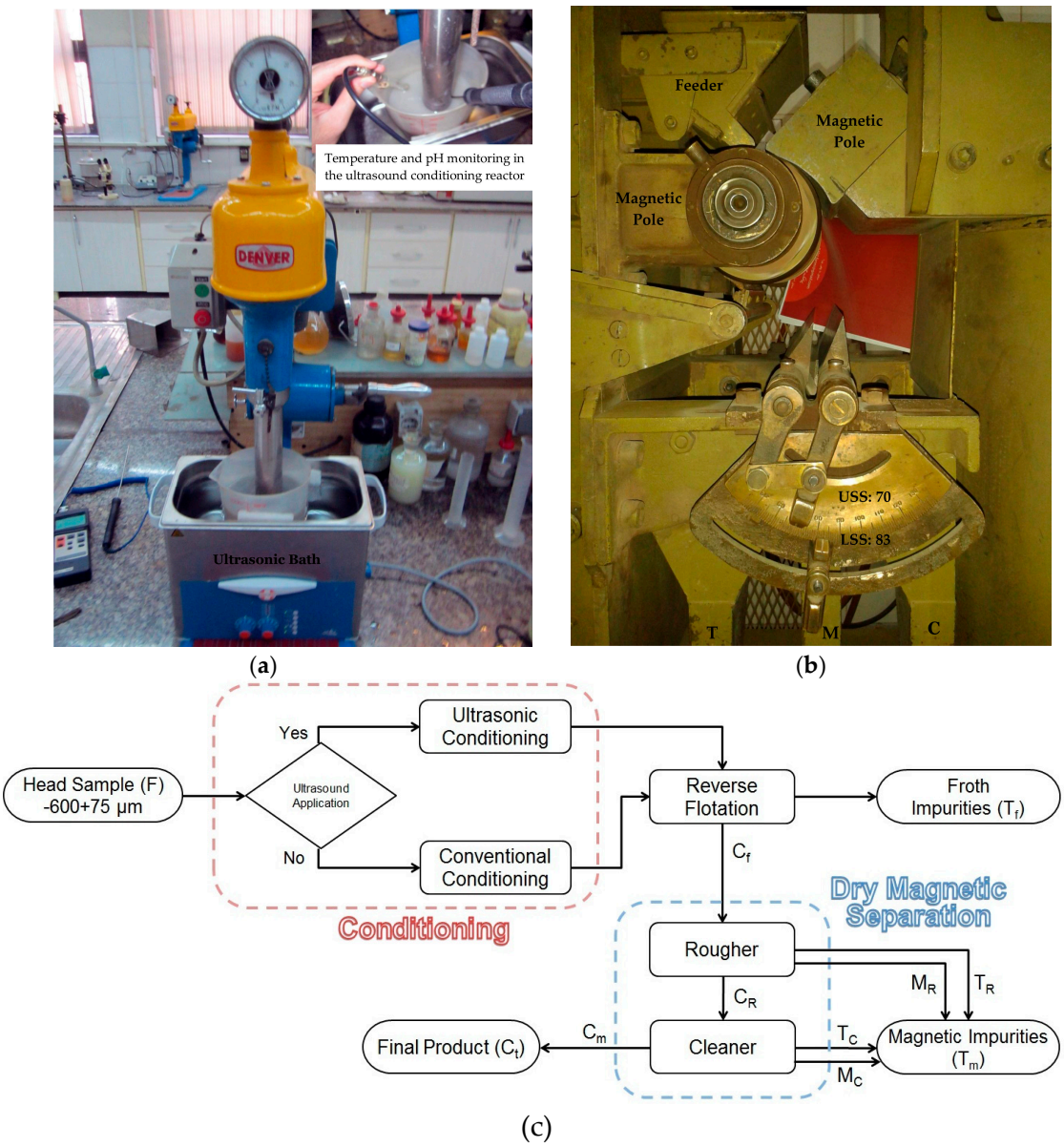

Figure 2. (**a**) Designed setup for conditioning with/without ultrasound irradiation for the reverse flotation experiments including monitoring of pH and temperature; (**b**) operating zone of the Exolon induced roll magnetic separator in the cleaner stage; and (**c**) schematic flowsheet for purification of silica, combining ultrasound irradiation with reverse flotation and magnetic separation.

Table 6. Operating conditions for dry high intensity magnetic separation tests and average weight of different streams.

Stage	SSA [1]		IMFI [2] (Tesla)	FR [3] (g/min)	RSIR [4] (rpm)	Consumed Power [5]		Weight (%) [6]		
	U	L				V	A	C	M	T
Rougher	70	84	1.5	95.1	86	98.4	4.9	91.40	6.14	2.46
Cleaner	70	83	1.7		75			94.24	4.73	1.02

[1] Separating Splitter Angles {Lower (L) for splitting C and M; Upper (U) for splitting M and T}; [2] Induced magnetic field intensity on roll prepared by changing of apparatus amperage and gaps between induced roll and magnetic pole pieces; [3] Feed Rate; [4] Rotation Speed of Induced Roll (rpm) measured by a DT2268 Lutron Tachometer; [5] V (Voltage), A (Amperage); [6] C (Non-magnetic), M (intermediate materials), T (Magnetic materials).

2.3. Measurements and Calculations

2.3.1. Calculation of Absorbed Ultrasound Power by the Slurry

The calorimetric approach was applied to calculate the absorbed power inside the reactor and tank while conditioning under indirect ultrasound irradiation. Equations (1) and (2) were employed to calculate the absorbed power by the solid and liquid in the reactor. Equations (3) and (4) were also employed to calculate the pure absorbed ultrasound power and the relevant ratio of transferred power to the reactor versus total produced power inside the ultrasonic bath, respectively.

$$P_S = \frac{\Delta Q_S}{\Delta t} = \frac{m_S C_S \Delta T}{\Delta t}, C_S = 0.84 J/(g.K) \quad (1)$$

$$P_L = \frac{\Delta Q_L}{\Delta t} = \frac{m_L C_L \Delta T}{\Delta t}, C_L = 4.1813 J/(g.K) \quad (2)$$

$$P_{PAU} = P_S + P_L - P_{Mech}, P_{Mech} = 13.69 Watt \quad (3)$$

$$E = \frac{P_{PAU}}{P_{Tank} + P_{PAU}} \times 100 \quad (4)$$

where

m_S and m_L: Available mass of solids and liquid in the sonication reactor;
C_S and C_L: Specific heat capacity of solids and liquid;
ΔT and Δt: Temperature change and duration of conditioning;
ΔQ_S and ΔQ_L: Absorbed heat by solids and liquid in the sonication reactor;
P_S and P_L: Absorbed power by solids and liquid in the sonication reactor;
P_{Mech}: Average absorbed power by the slurry due to rotor agitation;
P_{PAU} and P_{Tank}: Pure absorbed ultrasound power in the conditioning reactor and tank; and
E: Ratio of transferred power to the reactor versus the total produced power in the ultrasonic bath.

The total power consumption was monitored using a Wattmeter, which read 151.7 Watt for the entire volume of tank when the booster mode of the SW6H ultrasonic bath was selected. However, while the reactor was sitting inside the tank, the maximum filling capacity of the bath was reduced, which led to a loss of accessible power from 151.7 Watt down to a total absorbed power of 108.6 Watt. It is interesting to mention that the average absorbed ultrasound power to the available slurry in the reactor was 22.1 Watt, so the average ultrasonic intensity was 16.7 Watt per one liter of slurry.

2.3.2. Chemical Analysis and Calculation of Selectivity Index (S.I.)

According to Table 2, the silica and impurity grades of the head sample were based on the average grades measured by the chemical analyses (CA), which were selected due to their better accuracy and precision compared with the results of ICP-OES and XRF analyses. The two latter methods were imprecise when measuring SiO_2 and Al_2O_3 grades; CA is also recommended by various known standards for chemical analysis of silica powder [41–43]. It should be noted that the gravimetric method was used to measure SiO_2 and Al_2O_3, while both gravimetric and titration methods were employed during CaO measurement. To record accurate Fe_2O_3 and TiO_2 grades, Jenwey-6300 and Unico-2100 Spectrophotometers were used, while, for K_2O measurement a Jenwey-PFP flame photometer was utilized. The entire procedures followed were according to the ISO/IEC 17025:2005 standard.

Equations (5) and (6), respectively, were used for calculating silica recovery and impurity removal.

$$R_{Qtz} = \frac{c_{Qtz} \times C}{f_{Qtz} \times F} \times 100 \quad (5)$$

$$R_{waste} = (1 - \frac{c_{waste} \times C}{f_{waste} \times F}) \times 100 \quad (6)$$

where

R_{Qtz}: Recovery of silica in the concentrate;
R_{Waste}: Recovery of impurities (iron, alumina, titanium, calcium and so on) in the tailings;
C and F: Weight of concentrate and feed respectively;
c_{Qtz} and f_{Qtz}: Silica grade in the concentrate and feed respectively; and
c_{waste} and f_{waste}: Impurity grades (iron, alumina, titanium, calcium and so on) in the concentrate and feed, respectively.

In order to quantify and be able to compare the selectivity of reverse flotation and magnetic separation, Equation (7) (Gaudin's selectivity index) was used [44]. The selectivity Index (S.I.) is a number which expresses the overall selectivity of separation as follows:

$$S.I. = \sqrt{\frac{R_{Qtz} \times R_{waste}}{(100 - R_{Qtz}) \times (100 - R_{waste})}} \quad (7)$$

where

$S.I.$: Selectivity Index in a process;

For calculation of the selectivity index, the following conditions can occur:

a. No selectivity: R_{Waste} or $R_{Qtz} = 0$, then $S.I = 0$;
b. Ideal selectivity: $R_{Waste} = 100$ or $R_{Qtz} = 100$, then $S.I = \infty$;
c. No preferred selectivity: $R_{Waste} + R_{Qtz} = 100$, e.g.,$R_{Waste} = R_{Qtz} = 50$, then $S.I = 1$; and
d. Poor selectivity: $R_{Waste} + R_{Qtz} < 100$, especially when $R_{Waste} << R_{Qtz}$ then $S.I < 1$.

In addition, it should be noted that the historical data design (HDD) of DX7 software was utilized for modeling and optimizing the reverse flotation process.

3. Results and Discussions

3.1. Reverse Flotation

The detailed results of the reverse flotation experiments are shown in Table A1. In order to demonstrate the effect of indirect ultrasound irradiation (indirect sonication) on the performance of reverse flotation, eight pairs of experiments were selected and the most important responses were investigated. Figures 3 and 4 show the effect of ultrasound irradiation on grades of the flotation concentrate and Figure 5 shows the impact of ultrasound irradiation on removal performance of the major impurities. It should be noted that, regarding the C_4 and C_5 collectors, six different operating conditions are presented in Figures 5–11 using the following descriptions:

C_4_15_Na: Using C_4 at neutral pH with 15 min of conditioning
C_4_20_Na: Using C_4 at neutral pH with 20 min of conditioning
C_4_15_Ac: Using C_4 in an acidic environment with 15 min of conditioning
C_4_20_Ac: Using C_4 in an acidic environment with 20 min of conditioning
C_5_Na: Using C_5 at neutral pH with 30 min of conditioning
C_5_Ac: Using C_5 in an acidic environment with 30 min of conditioning
US: Ultrasound Irradiation
Nus: Non-ultrasound (Conventional)

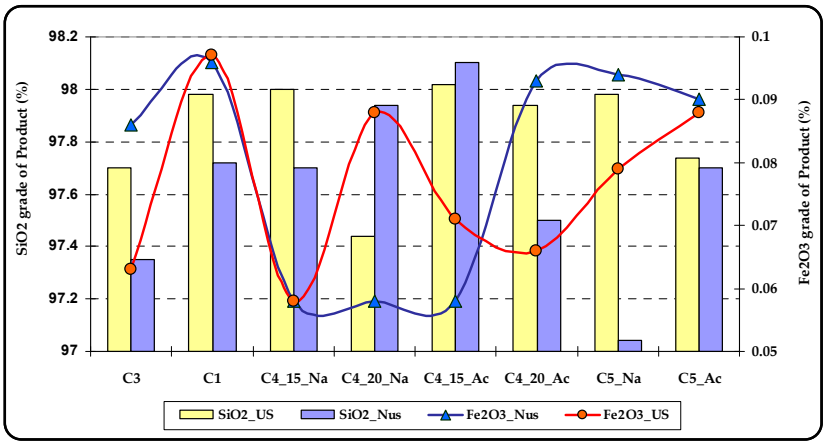

Figure 3. Effect of ultrasound irradiation on the SiO_2 and Fe_2O_3 grades of the flotation concentrate.

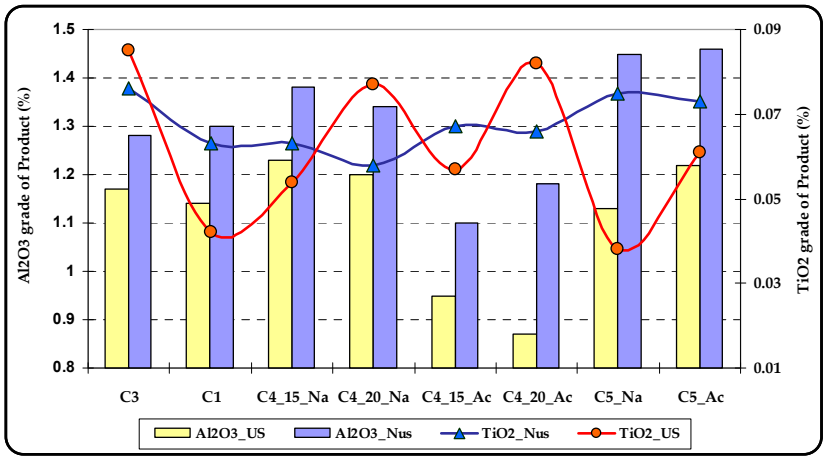

Figure 4. Effect of ultrasound irradiation on the Al_2O_3 and TiO_2 grades of the flotation concentrate.

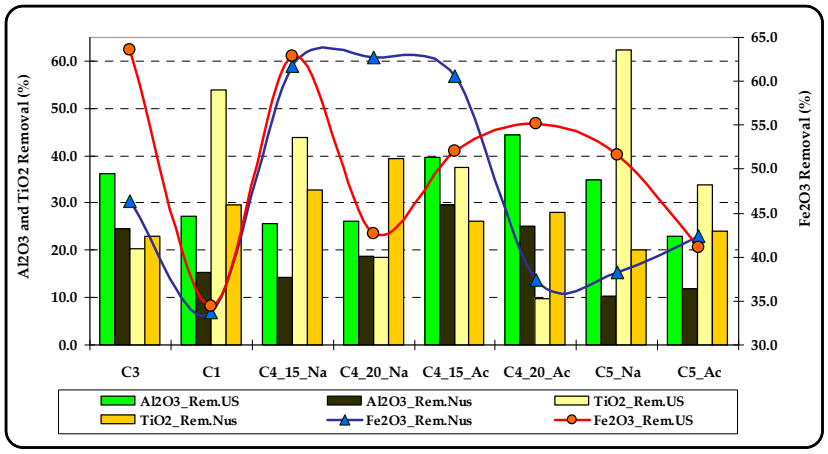

Figure 5. Effect of ultrasound irradiation on Al_2O_3, TiO_2 and Fe_2O_3 removal in reverse flotation.

According to Table A1 and considering Figures 3–5, the following conclusions can be drawn:

(1) As can be seen in most of these tests (6 pairs out of 8), ultrasound irradiation increased the silica grades and the highest grade was in the range of 98%–98.1%, which was achieved by using C_4 as the collector. Unlike the other two pairs, ultrasound irradiation during conditioning improved the removal of iron impurities compared to conventional conditioning.

(2) The lowest Fe_2O_3 grade of the silica concentrate at 0.058% and maximum iron removal was achieved by using C_4 as the collector with a total dosage of 2000 g/t. Collectors C_2 and C_3 were less effective while C_1 (sodium oleate) was the worst. Decreasing the collector dosage from 2000 g/t to 1200 g/t was not satisfactory for C_5.

(3) In all tests, when ultrasound irradiation was available, the Al_2O_3 grade of the concentrate was decreased; more specifically, the alumina removal increased from an average of 18.75% up to 32.1%. This phenomenon was due to detaching the clays from the surfaces of silica particles and flowing of the clays to the froth zone as entrainment.

(4) Application of C_1 or C_5 at neutral pH plus ultrasound irradiation during conditioning can be useful to decrease the TiO_2 grade of the concentrate down to below 0.05%.

(5) The best selectivity index for iron removal in reverse flotation was found in experiments 10 (C_4_Ac_15.Nus) and 13 (C_4_Ac_20.US), but only when the process finished with reverse flotation. The micro-attrition effect of ultrasound irradiation within the conditioning process resulted in better selectivity indices for Al_2O_3 and K_2O in experiment 13.

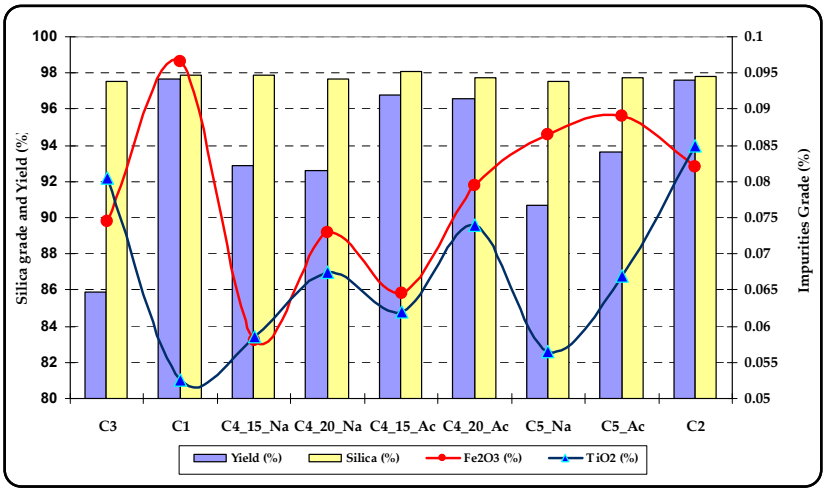

Figure 6. Effect of mixed collectors on yield, silica and impurity grades under different conditions.

In order to identify the most suitable collector by ignoring the presence or absence of ultrasound irradiation, Figure 6 shows the yield and product grades (SiO_2, Fe_2O_3 and TiO_2) versus mixed collectors under different conditions. Then, Figure 7 shows the effect of mixed collectors on silica recovery and impurity removal under different conditions. In addition, Figure 8 shows the effect of mixed collectors on the selectivity index of impurity removal under different conditions.

Considering Figures 6–8, the following outcomes can be summarized as below:

1. To reduce TiO_2 in the silica concentrate, the best collector was sodium oleate. In addition, this collector showed strong performance for removing carbonates and a weak efficiency for iron removal.
2. The best collector for iron removal was C_4. However, iron removal was higher in neutral pH than acidic pH. As a result of higher silica loss, optionally, acidic pH can be selected over neutral pH. In addition, the conditioning time of 15 min was better than 20 min in both neutral and acidic pH. It should be noted that the maximum Al_2O_3 removal was achieved with this collector and a conditioning of 15 min in an acidic environment.
3. The best collector to improve silica grade was C_4 with 15 min of conditioning at an acidic pH; the average SiO_2 grade reached 98.06%.

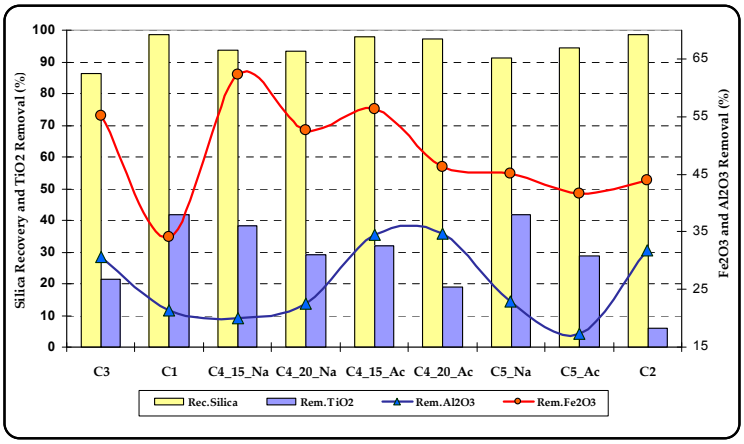

Figure 7. Effect of mixed collectors on silica recovery and impurity removal under different conditions.

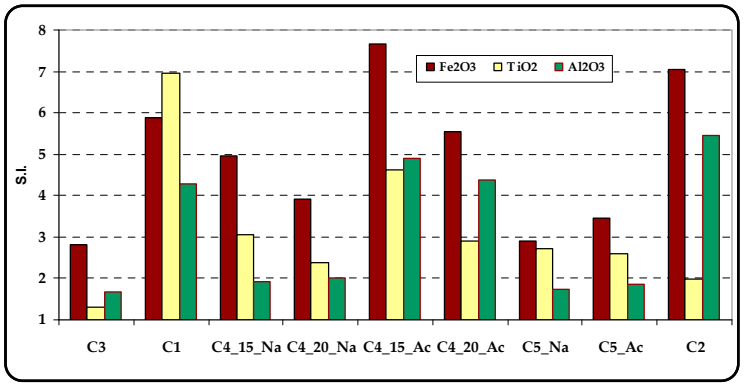

Figure 8. Effect of mixed collectors on the selectivity index of impurities under different conditions.

As a result, using C_4 was successful for removing iron impurities from low grade silica. Therefore, it is possible to say that the synergistic effects of mixing four collectors led to this successful result. It should be noted that C_4 had promising results that were better at neutral pH than acidic pH, therefore froth flotation using C_4 at neutral pH can be a cost effective approach to avoid acid usage and its relevant environmental problems in wastewater neutralization.

3.2. The Effect of Ultrasound Irradiation on Efficiency of Magnetic Separation

The product grades for different experiments using a two stage magnetic separation process are presented in Table A2. Figure 9 shows the effect of ultrasound irradiation on Fe_2O_3 removal and relevant selectivity indices in different experiments. According to Table A2, the average selectivity index for Fe_2O_3 removal was increased from 2.7 to 3.17 (17.4% relative improvement).

According to Table A2 and Figure 10, the Fe_2O_3 grade of the final product varied from 0.032% to 0.049%; the average Fe_2O_3 grade for experiments with ultrasound irradiation was 12.5% lower than for non-ultrasound experiments, which was a decrease from 0.04% to 0.035%. On the other hand, ultrasound irradiation in the conditioning phase of reverse flotation showed about a 14.9% improvement in iron removal with magnetic separation and consequently it increased from the average of 52.96% to 60.85%. The positive response of ultrasound irradiation on another downstream process (magnetic separation) was similar to the effect of attrition scrubbing on improvement of the iron removal efficiency in DHIMS, which was previously proven [7]. As a result, it can be concluded that ultrasound irradiation acts like micro-attrition scrubbing especially for detaching clays and other surface contaminants from silica particles. Therefore, surface cleaning of particles led to the better selectivity in magnetic separation.

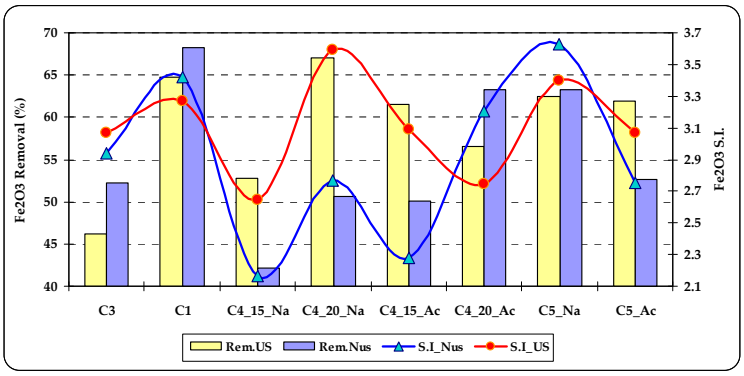

Figure 9. Effect of ultrasound irradiation on selectivity index and Fe_2O_3 removal in dry high intensity magnetic separation.

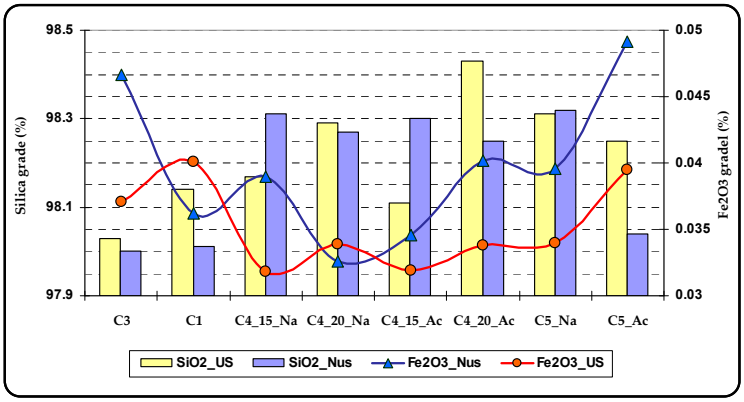

Figure 10. Effect of ultrasound irradiation on product grades for the silica purification flowsheet.

3.3. The Effect of Ultrasound Irradiation on Efficency of the Silica Purification Flowsheet

The detailed results for the flowsheet including reverse flotation and two levels of DHIMS are recorded in Table A2. As can be seen in Figure 10, in most of these tests (6 pairs out of 8), ultrasound irradiation increased the silica grades and the highest grade was 98.43%. Unlike the other two pairs, ultrasound irradiation during conditioning improved the removal of iron impurities compared to conventional conditioning.

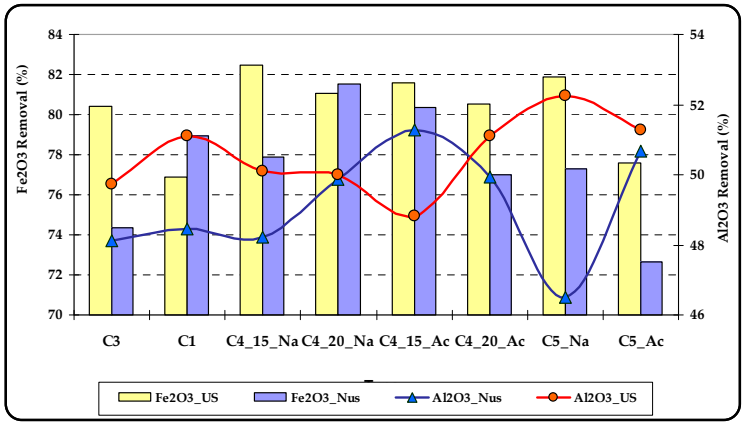

Figure 11. Effect of ultrasound irradiation on Fe_2O_3 and Al_2O_3 removal efficiency for the silica purification flowsheet.

In addition, Figure 11 shows the positive effect of ultrasound irradiation on removing Fe_2O_3 and Al_2O_3 from silica.

As can be seen in Table A2, in experiments using ultrasound irradiation, the SiO_2 and TiO_2 recoveries decreased slightly. However, the elimination rate of alumina and iron impurities increased and notably the increases were 3.1% (from 49.13% up to 50.66%) and 3.3% (from 77.51% up to 80.09%), respectively, while the silica loss was merely 1% due to indirect sonication. Consequently the average selectivity index for removing iron impurities was increased from 3.961 to 4.161.

According to Table A2, it can be concluded that experiments 12 (C_4_Ac_15.US), 13 (C_4_Ac_20.US) and 9 (C4_Na_20.Nus) had the highest selectivities for iron removal and these were 4.73, 4.59 and 4.48, respectively. Therefore, to consider indirect ultrasound irradiation in reverse flotation, the optimum condition was set at pH = 3.5, using C_4 with a conditioning duration of 15 or 20 min. When indirect ultrasound irradiation was not employed, 20 min conditioning and utilization of C_4 at neutral pH was the optimum point to remove iron impurities. Accordingly, it is possible to say that ultrasound irradiation can reduce the conditioning time from 20 down to 15 min resulting in a higher silica grade, a low amount of alumina in the final product and better iron removal selectivity in the silica purification flowsheet.

As a result, it can be concluded that all equipment in the pink box in Figure A1 can be replaced by a new enrichment circuit. This includes ultrasound irradiation in the conditioning phase of reverse flotation, followed by drying and a two stage dry high intensity magnetic separation process. Please note that future pilot tests should be performed to confirm its success in a continuous process.

3.4. Modeling and Optimization of Reverse Flotation Using C_4

C_4 was the best mix of collectors for iron removal from silica. Therefore eight tests (experiments 6 to 13) with relevant conditions and results were selected for modeling and optimizing reverse flotation, using this collector. It should be noted that the historical data design (HDD) of the DX7 software package was used for this purpose. There were three alternatives for considering ultrasound irradiation in the modeling as follow:

1. Non-quantified parameter: with/without ultrasound irradiation;
2. Application of total absorbed power in the sonication reactor;
3. Application of total absorbed power intensity (Watt/liter of slurry) in the sonication reactor.

The three alternatives above were inserted into the software and modeling was performed, separately. Then R-square (R^2), adjusted R^2, predicted R^2 and adequate precision were calculated for each response and the above three models were compared. Finally, the second alternative (total absorbed power in the sonication reactor), was selected as the best indication of indirect ultrasound irradiation and the design data are summarized in Table 7. The predicted linear coded models, with dimensionless variables following Equation (8), are reported in Table 8. It should be noted that when the coefficient (X_1, X_2, ... , X_7) is zero, it means that the relevant parameter was insignificant to predict the response. On the other hand, by looking at the coefficients presented in Table 8, the importance of each effect (positive or negative) can be easily determined. Afterwards, considering the actual factors, predicting formula for the product grades, silica recovery and impurities removal were developed as detailed in Equations 9–14, respectively.

$$Y_i = X_0 + X_1.A + X_2.B + X_3.C + X_4.AB + X_5.AC + X_6.BC + X_7.A^2 \quad (8)$$

where

Y_i: Response (i.e., silica and impurity grades, recovery and impurities removal); and
X_i: Coefficients for predicted coded or actual models.

Table 7. Variables, symbols and selected levels of HDD for reverse flotation using the C4 collector.

Variable Name	Unit	Symbol	Levels		Statistics			
			Low	High	Avg.	Min.	Max.	S.D.
pH	-	A	3.4	7.6	5.39	3.41	7.54	2.04
Conditioning Time [1]	min	B	15	20	17.50	15.00	20.00	2.67
Absorbed power [2]	Watt	C	5	45	26.55	9.99	43.42	13.72

[1] For collector with/without ultrasound irradiation; [2] Absorbed power = P_S + P_W.

Table 8. Predicted coded models for each response using the C4 collector.

Response		I [i]	Main Effects			Interactions and Curvature				Model	
			A	B	C	AB	AC	BC	A^2		
		Coefficients								R^2	AP [ii]
		X_0	X_1	X_2	X_3	X_4	X_5	X_6	X_7		
Yield		94.57	−2.25	0	0	0	0	0.89	0	0.961	17.45
G [iii]	SiO_2	92.50	0.79	0	−1.05	0	−1.46	0	6.72	0.926	8.28
	Fe_2O_3	0.40	−0.058	−0.002	0.071	0	0.097	−0.008	−0.42	0.999	72.59
	Al_2O_3	2.12	0	−0.028	0	0	0.27	−0.072	−1.18	0.980	15.91
	TiO_2	0.065	−0.004	0.0042	0.0053	−0.002	0	0.012	0	0.997	29.09
	CaO	2.27	−0.48	0	0.45	−0.048	0.55	−0.11	−2.67	0.999	31.74
	K_2O	0.27	0.12	0	0	0	0	0.093	0	0.797	7.79
R [iv]	SiO_2	97.42	−2.62	−0.34	0.56	0	0	1.07	−2.52	0.999	75.54
	Fe_2O_3	−170.46	39.91	1.18	−47.59	0	−65.34	5.08	284.47	0.999	44.20
	Al_2O_3	−25.71	0	1.81	0	0	−14.89	3.30	66.14	0.974	13.92
	TiO_2	30.47	6.06	−4.39	−5.81	2.30	0	−13.23	0	0.995	24.86
	CaO	−366.71	98.02	0	−92.86	9.96	−111.95	22.29	548.1	0.999	33.92
	K_2O	37.43	−25.80	0	0	0	0	−22.92	0	0.782	7.55

[i] Intercept; [ii] Adequate Precision; [iii] Grades; [iv] Recovery & impurities removal.

$$c_{Qtz} = 133.059 - 15.521A + 0.139C - 0.0348AC + 1.5244A^2 \quad (9)$$

$$c_{Fe_2O_3} = -2.166 + 0.965A + \frac{3.39}{1000}B - \frac{6.4}{1000}C + \frac{2.315}{1000}\mathrm{AC} - \frac{1.602}{10000}BC - 0.096A^2 \quad (10)$$

$$c_{TiO_2} = 0.1056 + \frac{4.558}{1000}A - \frac{2.1}{1000}B - \frac{3.813}{1000}\mathrm{C} - \frac{3.715}{10000}AB + \frac{2.329}{10000}\mathrm{BC} \quad (11)$$

$$R_{Qtz} = 98.0377 + 5.03A - 0.67\mathrm{B} - 0.346\mathrm{C} + 0.0214\mathrm{BC} - 0.571\mathrm{A}^2 \quad (12)$$

$$R_{Fe2O3} = 1558.072 - 651.663\mathrm{A} - 2.068\mathrm{B} + 4.399\mathrm{C} - 1.556\mathrm{AC} + 0.102\mathrm{BC} + 64.505\mathrm{A}^2 \quad (13)$$

$$R_{TiO_2} = -21.055 - 4.769\mathrm{A} + 2.453\mathrm{B} + 4.338\mathrm{C} + 0.437\mathrm{AB} - 0.265\mathrm{BC} \quad (14)$$

After modeling, in view of the maximum grade of silica and its recovery, as well as the maximum removal of iron impurities, the best condition was determined as 15–20 min conditioning using ultrasound irradiation in an acidic environment (pH = 3.5). When ultrasonic irradiation was not employed, the optimum condition was 20 min conditioning at neutral pH (pH = 7–7.5); this was already confirmed via the Fe_2O_3 selectivity index in Section 3.3.

According to Table 8 and Equations (9–14), the following highlights can be summarized:

1. The positive effect of interaction between conditioning time and absorbed power, including the negative effect of pH, is described as two influencing factors on flotation yield. One was that the quartz loss in the froth zone increases significantly with pH increase; and the other was increasing the flotation yield by increasing the conditioning time with indirect ultrasound irradiation.
2. The most important factor for prediction of the Fe_2O_3 grade in the flotation yield was a quadratic effect of pH. The other notable factors were the main effects (B and C) and interactions (AC and BC) which showed results of being less effective.
3. The quadratic effect of pH was the most important and effective factor in Fe_2O_3 removal. The efficiency of removing iron impurities was decreased in the pH range of 3.5–5 while it increased in the pH range of 5–7.5. In conclusion, the C_4 collector had the weakest capability in removing iron impurities at pH = 5.

4. The interaction between pH and absorbed power had a negative effect on Fe_2O_3 removal. Thus utilizing indirect ultrasound irradiation with 20 min of conditioning at neutral pH resulted in the lowest Fe_2O_3 removal (see Figure 3).
5. The most important factor influencing the silica grade of the flotation yield was the quadratic effect of pH. In contrast, the interaction between pH and absorbed power had a negative effect on silica grade in the flotation product. Consequently, it is better to carry out conditioning at neutral pH when ultrasound irradiation is not employed. However, there was a considerable positive effect of ultrasound irradiation on improving SiO_2 grade.
6. The interaction between conditioning time and absorbed power had a negative effect on TiO_2 grade in the flotation product. Therefore, in the presence of ultrasound irradiation and increase of conditioning time, the TiO_2 grade in the flotation product will consequently be increased.

3.5. Validation Tests and Discussion of Error in Reverse Flotation Using C_4

After modeling, in view of the maximum grade of silica as well as the minimum Fe_2O_3 and TiO_2 contents in the product, the optimum conditions were predicted as 15 min of conditioning at neutral pH by the DX7 software. The conditions of two predicted points were the same as experiments 6 and 7 reported in Table 5. Then, two replication tests were carried out for each of the above-mentioned experiments. Afterwards, the standard deviation (S.D.), confidence intervals (C.I.) and predicted intervals (P.I) were calculated for each response. The predicted responses and the results of the validation tests, including a summary of statistical calculations are summarized in Table 9. As can be seen in Table 9, the fluctuation of Fe_2O_3 and TiO_2 contents in the silica product was negligible in the presence of ultrasound irradiation during the conditioning phase of reverse flotation. It is interesting to say that in order to reach over 98% purity silica, the application of ultrasound irradiation is essential. It should be noted that the correlation coefficients of real responses (Avg.) versus predicted responses (Pred.) were over 0.99 for both states (with or without ultrasound irradiation).

Table 9. Results of validation tests, predicted values and summary of statistical calculations.

Description			Concentrate Weight and Grades (%)					Silica Recovery and Impurities Removal (%)			
			wt.	SiO_2	Fe_2O_3	Al_2O_3	TiO_2	SiO_2	Fe_2O_3	Al_2O_3	TiO_2
Validation Tests	US	Ex. 6	91.60	98.00	0.058	1.23	0.054	92.56	62.82	25.69	43.87
		Ex.6-Rep.1	89.40	97.92	0.057	1.27	0.045	90.26	64.33	25.12	54.35
		Ex.6-Rep.2	91.20	98.10	0.056	1.19	0.049	92.25	64.25	28.42	49.29
		Avg.	90.73	98.01	0.057	1.23	0.0493	91.69	63.80	26.41	49.17
		S.D.	1.172	0.090	0.001	0.040	0.0045	1.25	0.85	1.77	5.24
		95% PI-L	88.44	97.83	0.055	1.15	0.0405	89.25	62.13	22.95	38.90
		95% PI-H	93.03	98.18	0.059	1.31	0.0582	94.13	65.48	29.87	59.44
	Nus	Ex. 7	94.15	97.7	0.058	1.38	0.063	94.85	61.78	14.31	32.69
		Ex.7-Rep.1	91	97.55	0.062	1.35	0.075	91.53	60.51	18.98	22.55
		Ex.7-Rep.2	92.9	97.62	0.06	1.4	0.062	93.51	60.99	14.22	34.64
		Avg.	92.68	97.62	0.06	1.38	0.067	93.30	61.09	15.84	29.96
		S.D.	1.586	0.075	0.002	0.0252	0.0072	1.67	0.64	2.72	6.49
		95% PI-L	89.57	97.48	0.056	1.33	0.0525	90.03	59.84	10.50	17.24
		95% PI-H	95.79	97.77	0.064	1.43	0.0808	96.56	62.35	21.17	42.68
Predicted Values	US	Ex.6-Pred.	91.83	98.07	0.0578	1.24	0.0545	92.54	63.03	23.74	43.08
		95% CI-L	90.94	97.78	0.0517	1.14	0.0507	92.20	55.76	17.65	37.64
		95% CI-H	92.73	98.36	0.0639	1.33	0.0584	92.87	70.30	29.83	48.52
		95% PI-L	90.21	97.63	0.0489	1.09	0.0485	92.03	52.36	13.79	34.61
		95% PI-H	93.46	98.51	0.0668	1.39	0.0605	93.04	73.70	33.68	51.55
	Nus	Ex.7-Pred.	93.41	97.79	0.0567	1.37	0.0624	94.78	62.73	15.24	33.59
		95% CI-L	92.68	97.54	0.0506	1.26	0.0588	94.45	55.46	8.16	28.45
		95% CI-H	94.13	98.03	0.0628	1.48	0.0660	95.12	70.01	22.32	38.72
		95% PI-L	91.87	97.37	0.0478	1.21	0.0566	94.28	52.06	4.66	25.31
		95% PI-H	94.94	98.20	0.0657	1.53	0.0683	95.29	73.41	25.82	41.86

Ex.: Experiment; Rep.: Replication test; Avg.: Average; S.D.: Standard deviation; US: Conditioning with ultrasound irradiation; Nus: Conventional Conditioning; 95% CI-L: Low value of 95% confidence interval; 95% CI-H: High value of 95% confidence interval; 95% PI-L: Low value of 95% prediction interval; 95% PI-H: High value of 95% prediction interval.

3.6. Discussion about pH Effect in Reverse Flotation using Anionic Collectors

Several authors investigated the iron oxide–quartz flotation system, using anionic collectors with different functional groups of sulfate, sulfonate, hydroxamate, and carboxylates (lauric and oleic acids), and also cationic amine collectors. Such collectors can be used only with knowledge of the point of zero charge (PZC) for the minerals in question [14,45,46]. In general, the flotation responses as a function of pH are in good agreement with the electrical nature of the surfaces where the anionic and cationic collectors float the oxides at a pH region below and above the PZC of the minerals, respectively [45]. The PZC of quartz occurs in an acidic environment (at pH=2–3) while the PZC of goethite, hematite and limonite occurs at neutral or alkaline pH at around 6.7, 7 and 7–8, respectively [45,46]. Because the PZCs of hematite, goethite, and limonite are very close, therefore their flotation responses are similar with anionic and cationic collectors [45,46]. Former works showed an impressive iron removal from silica and feldspar by mixing sulfonate series collectors (Aero 801, 825 and 845) [14,15,47]. Other research showed that sodium oleate could be an appropriate collector for removing iron impurities from silica in the pH range of 5–7 [13,39], and applying sodium oleate in the pH range of 6.5–10.5 leading to best floatability of limonite [48]. Goethite can be floated very well until pH = 5.5 by sulfonate while hematite can be floated away from quartz with sulfonate in an acidic medium (pH = 2–4) or sodium oleate at a pH in the range of 6–8; Oleic acid showed good floatability of hematite in the pH range of 6.7–7.5 [45,46]. Former research proved that electrostatic adsorption between oleate and limonite, and hydrogen bonding between oleic molecules and limonite are the major mechanisms in a pH range of 2.0–4.0 while in the pH range of 4.0–10.5, chemical reaction between oleate and iron plays the dominant role, and the infrared spectroscopic analysis showed that the reaction product of sodium oleate and limonite should be ferrous oleate [48]. In addition, the dominant mechanism for floatability of hematite at neutral pH (6.7–7.5) with oleic acid was chemisorption on surface sites [45,46]. As a result, it can be concluded that conditioning in an acidic environment (pH = 3.5) or neutral pH (pH = 7–7.5) are two optimum pH regions, whereas the target is removing iron impurities from silica in reverse flotation by using anionic collectors. Therefore, the quadratic effect of pH on iron removal performance was a logical phenomenon, when C_4 was applied as an anionic mixed collector.

4. Conclusions

In this research work, the application of indirect ultrasound irradiation within the conditioning phase of reverse flotation on a relatively low grade silica sample was thoroughly investigated. The silica product of flotation tests was dried then treated in two stages of dry high intensity magnetic separation. This work, clearly demonstrated the advantages and disadvantages of ultrasound irradiation on purification of silica. In addition, it should be noted that in order to supply suitable raw material for colorless glass manufacturing, a combination of reverse flotation and dry high intensity magnetic separation should be the best approach for beneficiation of low grade silica deposits. Some of the outcomes of this study are outlined as follows:

1. Ultrasound irradiation has a significant effect on the conditioning phase of flotation. Neutral pH is affected by ultrasonic waves caused by collapse of cavitation bubbles and generation of free radicals by changing the pH which mainly depends on the types of consumed reagents and increasing temperature in the sonication reactor. In the presence of ultrasound irradiation, during conditioning, the average rate of increasing temperature was 0.46 °C per minute and just slightly 2.5 times more than conventional conditioning. The average rate of increasing temperature was 0.19 °C per minute in conventional conditioning.
2. When the experiment was carried out using ultrasound irradiation, silica grade increased. The yield and alumina grade of the concentrate decreased compared to the same conditions without ultrasound irradiation. This phenomenon was due to detaching clays from the surfaces of silica particles and the clays flowed to the froth zone as entrainment. It was concluded that ultrasound irradiation acts like a micro-attrition scrubber and was a powerful

tool, not only for resolving clays problems in flotation but also for improving the selectivity of downstream processes.

3. Excessive ultrasound irradiation during conditioning was harmful to iron impurities removal from silica in reverse flotation. However, this excessive sonication (longer than 20 min), improved the removal of Al_2O_3 and K_2O by detachment of clays from silica particles.
4. Ultrasound irradiation plays an important role in the selectivity of impurity removal (especially iron and clays) from silica in reverse flotation, including downstream processes.
5. The lowest Fe_2O_3 grade of the flotation product was 0.058% and this was achieved using 2000 g/t of C_4 as the collector. C_4 consisted of Aero 801, Aero 825, oleic acid and sodium oleate at equal dosage. It should be noted that the mixture of these collectors had promising results, which were better at neutral pH than acidic pH. Therefore, reverse flotation using C_4 at neutral pH can be a cost effective approach to avoid acid usage and all the relevant environmental problems in wastewater neutralization.

Acknowledgments: The authors of this paper would like to express their sincere thanks to the mineral processing laboratory at the University of Tehran for the supply of reagents and equipment. The kind support of the Kaveh Glass Industrial Group for supply of silica samples, information from a processing line and also chemical analyses of samples is gratefully acknowledged. In addition, the support of the Iranian Mineral Processing Research Center (IMPRC) for XRF analyses of samples and Golnaz Jozanikohan for implementation and interpretation of XRD analyses is highly appreciated. Finally, special thanks are given to Anthony Douglas Farmer for his valuable scientific advice about ultrasound irradiation in the mineral industry and Mahdi Shevrini for his technical comments on silica processing and glass manufacturing.

Author Contributions: Hamed Haghi conceived and designed the experiments, developed the setup for indirect ultrasound irradiation in the conditioning phase of flotation, performed the experiments, analyzed the data and wrote the paper under the supervision and guidance of Mohammad Noaparast and Sied Ziaedin Shafaei Tonkaboni with consultation from Mirsaleh Mirmohammadi. Mirsaleh Mirmohammadi performed the mineralogical studies. All authors contributed to the interpretation of results, discussions and conclusions.

Conflicts of Interest: The authors declare no conflict of interest.

Appendix A

Table A1. Results of reverse flotation experiments under different conditions with/without ultrasound irradiation.

No.	Concentrate Weight and Grades (%)							Silica Recovery & Impurities Removal (%)					
	C_f	SiO_2	Fe_2O_3	Al_2O_3	TiO_2	CaO	K_2O	SiO_2	Fe_2O_3	Al_2O_3	TiO_2	CaO	K_2O
1	89.19	97.35	0.086	1.28	0.076	0.54	0.17	89.5	46.3	24.7	23.1	-	62.3
2	82.65	97.7	0.063	1.17	0.085	0.66	0.1	83.3	63.6	36.2	20.3	-	79.4
3	97.60	97.83	0.082	1.06	0.085	0.49	0.12	98.5	44.0	31.8	5.9	-	70.9
4	96.68	97.98	0.097	1.14	0.042	0.02	0.41	97.7	34.4	27.3	53.9	95.9	1.4
5	98.65	97.72	0.096	1.3	0.063	0.1	0.39	99.4	33.7	15.4	29.5	78.9	4.3
6	91.60	98.0	0.058	1.23	0.054	0.02	0.33	92.6	62.8	25.7	43.9	96.1	24.8
7	94.15	97.7	0.058	1.38	0.063	0.04	0.39	94.8	61.8	14.3	32.7	91.9	8.7
8	93.17	97.44	0.088	1.2	0.077	0.04	0.42	93.6	42.6	26.3	18.6	92.0	2.7
9	92.00	97.94	0.058	1.34	0.058	0.02	0.37	92.9	62.7	18.7	39.5	96.1	15.3
10	97.09	98.1	0.058	1.1	0.067	0.05	0.35	98.2	60.6	29.6	26.2	89.6	15.5
11	96.09	97.5	0.093	1.18	0.066	0.47	0.085	96.6	37.5	25.2	28.0	3.2	79.7
12	96.47	98.02	0.071	0.95	0.057	0.35	0.075	97.5	52.1	39.6	37.6	27.6	82.0
13	97.01	97.94	0.066	0.87	0.082	0.3	0.089	98.0	55.2	44.3	9.7	37.6	78.5
14	93.86	97.04	0.094	1.45	0.075	0.01	0.1	93.9	38.3	10.2	20.1	98.0	76.7
15	87.52	97.98	0.079	1.13	0.038	0.17	0.072	88.4	51.6	34.8	62.3	68.1	84.3
16	91.53	97.7	0.09	1.46	0.073	0.17	0.074	92.2	42.3	11.9	24.2	66.7	83.2
17	95.70	97.74	0.088	1.22	0.061	0.41	0.076	96.4	41.1	23.0	33.8	15.9	81.9
NU	94.07	97.63	0.079	1.31	0.068	0.12	0.24	94.7	47.9	18.8	27.9	74.9	43.2
S.D.	3.13	0.33	0.018	0.13	0.006	0.16	0.15	3.3	12.0	7.0	6.1	33.4	35.2
US	93.16	97.85	0.077	1.11	0.065	0.15	0.19	94.0	49.7	32.1	31.8	61.9	56.2
S.D.	5.24	0.20	0.013	0.09	0.018	0.17	0.16	5.3	10.4	5.9	19.0	35.9	37.2

NU: Average amount for all tests without ultrasound irradiation during conditioning; S.D.: Standard deviation; US: Average amount for all tests with ultrasound irradiation during conditioning.

Table A2. Summary of results for a flowsheet including reverse flotation and two stages of DHIMS.

No.		C_T	Grades (%)				Recovery & Impurities Removal				Selectivity Index		
			SiO_2	Fe_2O_3	Al_2O_3	TiO_2	SiO_2	Fe_2O_3	Al_2O_3	TiO_2	Fe_2O_3	Al_2O_3	TiO_2
1		78.67	98.00	0.047	1.00	0.050	79.5	74.3	48.1	55.4	3.35	1.90	2.19
2		75.46	98.03	0.037	1.01	0.050	76.3	80.4	49.7	57.2	3.63	1.78	2.07
3		82.57	98.07	0.037	0.89	0.050	83.5	78.5	51.5	53.2	4.30	2.32	2.40
4		82.37	98.14	0.040	0.90	0.040	83.4	76.9	51.1	62.6	4.08	2.29	2.90
5		83.13	98.01	0.036	0.94	0.050	84.0	78.9	48.5	52.8	4.44	2.22	2.43
6		78.82	98.17	0.032	0.96	0.050	79.8	82.5	50.1	55.3	4.31	1.99	2.21
7		80.97	98.31	0.039	0.97	0.050	82.1	77.9	48.2	54.1	4.02	2.06	2.32
8		79.79	98.29	0.034	0.95	0.050	80.9	81.1	50.0	54.7	4.25	2.06	2.26
9		80.86	98.27	0.033	0.94	0.040	81.9	81.6	49.9	63.3	4.48	2.12	2.80
10		81.16	98.30	0.035	0.91	0.050	82.3	80.4	51.3	54.0	4.35	2.21	2.33
11		81.65	98.25	0.040	0.93	0.041	82.7	77.0	49.9	62.0	4.01	2.18	2.80
12		82.54	98.11	0.032	0.94	0.051	83.5	81.6	48.8	52.2	4.73	2.20	2.35
13		82.36	98.43	0.034	0.90	0.051	83.6	80.5	51.1	52.3	4.59	2.31	2.37
14		81.92	98.32	0.040	0.99	0.050	83.1	77.3	46.5	53.5	4.08	2.06	2.38
15		76.21	98.31	0.034	0.95	0.035	77.3	81.9	52.3	69.7	3.92	1.93	2.80
16		79.55	98.04	0.049	0.94	0.041	80.4	72.7	50.7	63.0	3.30	2.05	2.64
17		81.17	98.25	0.040	0.91	0.049	82.2	77.6	51.3	54.9	4.00	2.21	2.37
NU	Avg.	80.99	98.19	0.040	0.95	0.047	82.0	77.5	49.1	57.3	3.96	2.10	2.47
	S.D.	1.38	0.14	0.006	0.03	0.005	1.44	2.94	1.58	4.63	0.46	0.11	0.23
US	Avg.	80.14	98.20	0.035	0.93	0.047	81.2	80.1	50.7	56.9	4.16	2.10	2.38
	S.D	2.78	0.13	0.003	0.04	0.006	2.83	1.98	1.06	5.76	0.34	0.19	0.27

C_T: Concentrate weight (%); NU: Average amount for all tests without ultrasound irradiation; Avg.: Average; S.D.: Standard deviation; US: Average amount for all tests with ultrasound irradiation.

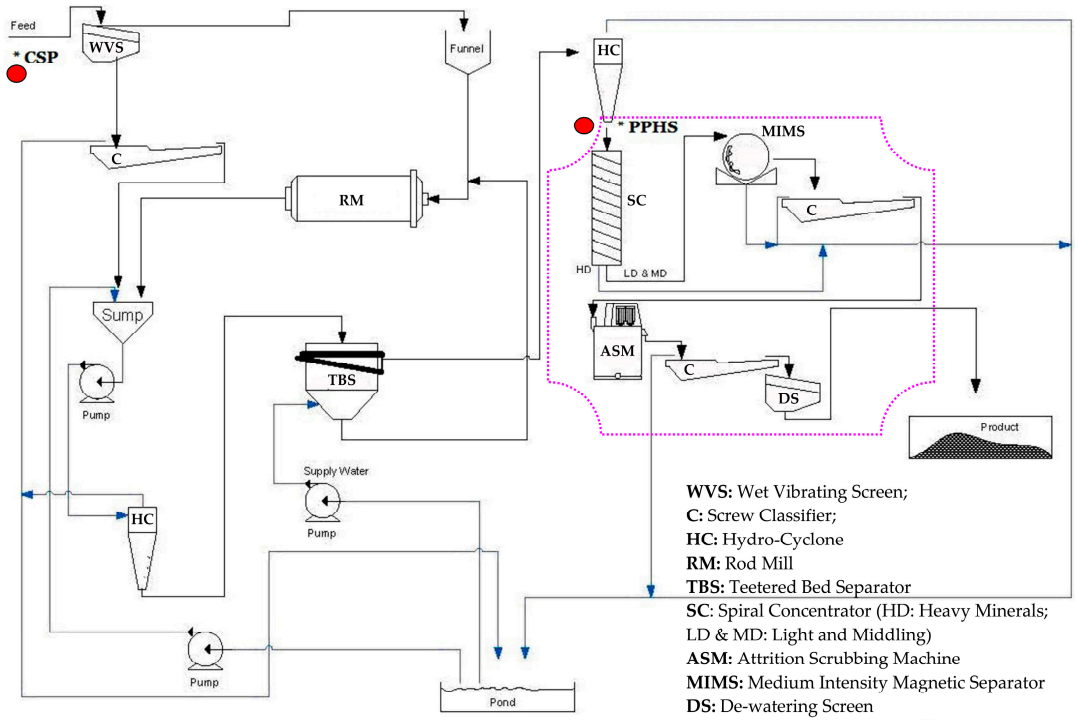

Figure A1. Flow sheet of the silica processing plant and points of sampling [4].

References

1. Bulatovic, S.M. Beneficiation of Silica Sand. In *Handbook of Flotation Reagents: Chemistry Theory and Practice*, 1st ed.; Elsevier: Amsterdam, The Netherlands, 2015; Volume 3, pp. 121–127.
2. BSI. *Methods for Sampling and Analysis of Glass-Making Sands*; BS 2975:1988; BSI: London, UK, 1988.
3. Shevrini, M.; Haghi, H. Modification of classifying unit in a silica plant using replacement of trommel screens with Teetered Bed Separator. In Proceedings of the XV Balkan Mineral Processing Congress, Sozopol, Bulgaria, 12–16 June 2013; Volume 1, pp. 524–529.

4. Shevrini, M.; Haghi, H. Improvement in product of silica plant by modification of size classifying unit and application of attrition scrubber. In Proceedings of the XXVII International Mineral Processing Congress, Santiago, Chile, 20–24 October 2014; pp. 147–158.
5. Raghu Kumar, C.; Tripathy, S.K.; Mohanan, S.; Venugopalan, T.; Suresh, N. Evaluation of floatex density separator performance using silica sand. In Proceedings of the XI International Seminar on Mineral Processing Technology, NML Jamshedpur, India, 15–17 December 2010; pp. 701–706.
6. Haghi, H.; Noaparast, M. Application of hot acidic scrubbing and hot agitated leaching for iron removal from Shenin silica mine (used in glass Industry). In Proceedings of the 13th Conference on Environment and Mineral Processing, Ostrava, Czech Republic, 4–6 June 2009; Volume IV, pp. 121–130.
7. Haghi, H.; Noaparast, M.; Ghorbani, A. Reduction of iron content from silica sand by scrubbing process. In Proceedings of the 11th International Mineral Processing Symposium, Belek-Antalya, Turkey, 21–23 October 2008; pp. 259–265.
8. Hearn, S.; Sadowski, J. Advances in the application of spiral concentrators for production of glass sand. In *Advances in Gravity Concentration*, 1st ed.; Honaker, R.Q., Forrest, W.R., Eds.; Society of Mining, Metallurgy, and Exploration, Inc. (SME): Englewood, CO, USA, 2003; pp. 179–187.
9. Ibrahim, S.S.; Selim, A.Q.; Hagrassc, A.A. Gravity separation of silica sands for value addition. *Part. Sci. Technol.* **2013**, *31*, 590–559. [CrossRef]
10. Al-Maghrabi, M.N.N.H. Improvement of low grade silica sand deposits in Jeddah area. *JKAU: Eng. Sci.* **2004**, *15*, 113–128. [CrossRef]
11. Haghi, H.; Noaparast, M. Iron removal from relatively low grade silica using magnetic separation. In Proceedings of the XXVII International Mineral Processing Congress, Santiago, Chile, 20–24 October 2014; pp. 84–93.
12. Andrews, P.R.A.; Collings, R.K. Canadian silica resources for glass and foundry sand production: Processing studies at CANMET. *Int. J. Miner. Process.* **1989**, *25*, 311–317. [CrossRef]
13. Goktepe, F.; Ipek, H.; Goktepe, M. Beneficiation of quartz waste by flotation and by ultrasonic treatment. *Physicochem. Probl. Miner. Process.* **2011**, *47*, 41–50.
14. Haghi, H.; Noaparast, M.; Ghadyani, A.; Ghorbani, A. Reduction of iron content from Shenin silica mine by reverse flotation. In Proceedings of the XII International Mineral Processing Symposium, Nevsehir, Turkey, 6–8 October 2010; pp. 465–474.
15. Hacifazlioglu, H. Enrichment of silica sand ore by cyclojet flotation cell. *Sep. Sci. Technol.* **2014**, *49*, 1623–1632. [CrossRef]
16. Teodorescu, E.; Sarachie, I.; Prida, T.; Ivan, I.; Popa, T. Glass sand production by flotation and magnetic separation technology. In Proceedings of the 7th International Mineral Processing Symposium (Innovations in Mineral and Coal Processing), Istanbul, Turkey, 15–17 September 1998; pp. 339–341.
17. Taxiarchou, M.; Panias, D.; Douni, I.; Paspaliaris, I.; Kontopoulos, A. Removal of iron from silica sand by leaching with oxalic acid. *Hydrometallurgy* **1997**, *46*, 215–227. [CrossRef]
18. Veglió, F.; Passariello, B.; Barbaro, M.; Plescia, P.; Marabini, A.M. Drum leaching tests in iron removal from quartz using oxalic and sulphuric acids. *Int. J. Miner. Process.* **1998**, *54*, 183–200. [CrossRef]
19. Veglió, F.; Passariello, B.; Abbruzzese, C. Iron removal process for high purity silica sands production by oxalic acid leaching. *Ind. Eng. Chem. Res.* **1999**, *38*, 4443–4448. [CrossRef]
20. Tarasova, I.I.; Dudeney, A.W.L.; Pilurzu, S. Glass sand processing by oxalic acid leaching and photocatalytic effluent treatment. *Miner. Eng.* **2001**, *14*, 639–646. [CrossRef]
21. Banza, A.N.; Quindt, J.; Gock, E. Improvement of the quartz sand processing at Hohenbocka. *Int. J. Miner. Process.* **2006**, *79*, 76–82. [CrossRef]
22. Haghi, H.; Noaparast, M.; Ghadyani, A.; AmiriParian, A. Investigation of the various processes of acidic leaching for iron removal from silica with statistical methods. In Proceedings of the XIIIth Balkan Mineral Processing Congress, Bucharest, Romania, 14–17 June 2009; Volume 1, pp. 297–305.
23. Haghi, H.; Ghadyani, A.; Faramarzi, M. Application of agitated leaching for iron removal from silica using sulfuric and hydrochloric acid. In Proceedings of the XXV International Mineral Processing Congress, Brisbane, Australia, 6–10 September 2010; pp. 325–334.
24. Farmer, A.D.; Collings, A.F.; Jameson, G.J. Effect of ultrasound on surface cleaning of silica particles. *Int. J. Miner. Process.* **2000**, *60*, 101–113. [CrossRef]
25. Collings, A.F.; Farmer, A.D. Enhanced leaching through the use of power ultrasound. In Proceedings of the 7th Mill Operators' Conference, Kalgoorlie, WA, Australia, 12–14 October 2000; pp. 273–276.

26. Collings, A.F.; Farmer, A.D.; Struthers, A.A. The effect of power ultrasound in the production of synthetic rutile by the becher process. In Proceedings of the 3rd International Heavy Minerals Conference, Fremantle, WA, Australia, 18–19 June 2001; pp. 235–240.
27. Aldrich, C.; Feng, D. Effect of ultrasonic preconditioning of pulp on the flotation of sulphide ores. *Miner. Eng.* **1999**, *12*, 701–707. [CrossRef]
28. Ozkan, S.G. Beneficiation of magnesite slimes with ultrasonic treatment. *Miner. Eng.* **2002**, *15*, 99–101. [CrossRef]
29. Ozkan, S.G.; Kuyumcu, H.Z. Investigation of mechanism of ultrasound on coal flotation. *Int. J. Miner. Process.* **2006**, *81*, 201–203. [CrossRef]
30. Ozkan, S.G.; Kuyumcu, H.Z. Design of a flotation cell equipped with ultrasound transducers to enhance coal flotation. *Ultrason. Sonochem.* **2007**, *14*, 639–645. [CrossRef] [PubMed]
31. Ozkan, S.G. Effects of simultaneous ultrasonic treatment on flotation of hard coal slimes. *Fuel* **2012**, *93*, 576–580. [CrossRef]
32. Cilek, E.C.; Ozgen, S. Effect of ultrasound on separation selectivity and efficiency of flotation. *Miner. Eng.* **2009**, *22*, 1209–1217. [CrossRef]
33. Celik, M.S. Effect of ultrasonic treatment on the floatability of coal and galena. *Sep. Sci. Technol.* **1989**, *24*, 1159–1166. [CrossRef]
34. Ambedkar, B.; Nagarajan, R.; Jayanti, S. Ultrasonic coal-wash for de-sulfurization. *Ultrason. Sonochem.* **2011**, *18*, 718–726. [CrossRef] [PubMed]
35. Farmer, A.D.; Collings, A.F.; Jameson, G.J. The application of power ultrasound to the surface cleaning of silica and heavy mineral sands. *Ultrason. Sonochem.* **2000**, *7*, 243–247. [CrossRef]
36. Zhao, H.L.; Wang, D.X.; Cai, Y.X.; Zhang, F.C. Removal of iron from silica sand by surface cleaning using power ultrasound. *Miner. Eng.* **2007**, *20*, 816–818. [CrossRef]
37. Mills, H.N. Glass raw materials. In *Industrial Minerals and Rocks*, 5th ed.; Lefond, S.J., Ed.; Society of Mining Engineers: New York, NY, USA, 1983; pp. 339–351.
38. Krukowski, S.T. Specialty Silica Materials. In *Industrial Minerals and Rocks, Commodities, Markets and Uses*, 7th ed.; Kogel, J.E., Trivedi, N.C., Barker, J.M., Krukowski, S.T., Eds.; Society of Mining, Metallurgy, and Exploration, Inc. (SME): Englewood, CO, USA, 2006; p. 842.
39. Chammas, E.; Panias, D.; Taxiarchou, D.; Anastassakis, G.N.; Paspaliaris, I. Removal of iron impurities and other major impurities from silica sand for the production of high added value materials. In Proceedings of the 9th Balkan Mineral Processing Congress, Istanbul, Turkey, 11–13 September 2001.
40. Bouabdallah, S.; Bounouala, M.; Chaib, A.S. Removal of iron from sandstone by magnetic separation and leaching: Case of El-Aouana. *J. Min. Sci.* **2015**, *22*, 33–44.
41. ASTM International. *Standard Test Methods for Chemical Analysis of Glass Sand*; ASTM C146-94a; ASTM International: West Conshohocken, PA, USA, 2014.
42. BSI. *Sampling and Analysis of Glass-Making Sands, Part 2: Methods for Chemical Analysis*; BS 2975-2:2008; BSI: London, UK, 2008.
43. Bureau of Indian Standards. *Chemical Analysis of Quartzite and High Silica Sand*; IS.1917 (7 Parts; 1991-2); Bureau of Indian Standards: New Delhi, India.
44. Vasanthakumar, B.; Ravishankar, H.; Subramanian, S. A novel property of DNA—As a bioflotation reagent in mineral processing. *PLoS ONE* **2012**, *7*, e39316. [CrossRef] [PubMed]
45. Fuerstenau, M.C.; Jameson, G.; Yoon, R.H. *Froth flotation: A Century of Innovation*; Society for Mining, Metallurgy, and Exploration: Littleton, CO, USA, 2007.
46. Somasundaran, P.; Moudgil, B.M. *Reagents in Mineral Technology*; Marcel Dekker Inc.: New York, NY, USA, 1989; Volume 27.
47. Ghorbani, A.; Haghi, H. Iron removal from Choghaie feldspar mine by flotation. In Proceedings of the 7th International Industrial Minerals Symposium and Exhibition, Kusadasi, Turkey, 25–27 February 2009.
48. Xie, X.Z.; Wang, Y.H. Effective collectors for limonite flotation and mechanism there in. *Min. Metall. Eng.* **2011**, *31*, 49–52.